International Compressor Engineering Conference   School of Mechanical Engineering

2016

Design Methodology Improvements of a Rotating Spool Compressor using a Comprehensive Model

Craig R Bradshaw
Torad Engineering, United States of America, craig.bradshaw@toradengineering.com

Greg Kemp
Torad Engineering, United States of America, greg.kemp@toradengineering.com

Joe Orosz
Torad Engineering, United States of America, joe.orosz@toradengineering.com

Eckhard A Groll
Purdue University, United States of America, groll@purdue.edu

Follow this and additional works at: https://docs.lib.purdue.edu/icec

Design Methodology Improvements of a Rotating Spool Compressor using a Comprehensive Model

Craig R. BRADSHAW[1*], Greg KEMP[1], Joe OROSZ[1], Eckhard A. GROLL[2]

[1] TORAD Engineering,
Cumming, GA, USA
ph. 770-889-8400, craig.r.bradshaw@gmail.com

[2] Ray W. Herrick Laboratories, School of Mechanical Engineering at Purdue University,
West Lafayette, IN, USA
groll@purdue.edu

* Corresponding Author

ABSTRACT

An improvement to the design process of the rotating spool compressor is presented. This improvement utilizes a comprehensive model to explore two working fluids (R410A and R134a), various displaced volumes, at a variety of geometric parameters. The geometric parameters explored consists of eccentricity ratio and length-to-diameter ratio. The eccentricity ratio is varied between 0.81 and 0.92 and the length-to-diameter ratio is varied between 0.4 and 3. The key tradeoffs are evaluated and the results show that there is an optimum eccentricity and length-to-diameter ratio, which will maximize the model predicted performance, that is unique to a particular fluid and displaced volume. For R410A the modeling tool predicts that the overall isentropic efficiency will optimize at a length-to-diameter ratio that is lower than for R134a. Additionally, the tool predicts that as the displaced volume increases the overall isentropic efficiency will increase and the ideal length-to-diameter ratio will shift. The result from this study are utilized to develop a basic design for a 141 kW (40 tonsR) capacity prototype spool compressor for light-commercial air-conditioning applications.

1. INTRODUCTION

The rotating spool compressor is a novel rotary compressor mechanism most similar to the sliding vane compressor. Primary differences are described by Kemp et al. (2008) and include three key differences from a sliding vane compressor, as shown in Figure 1.

- The vane is constrained by means of an eccentric cam allowing its distal end to be held in very close proximity to the housing bore while never contacting the bore.

- The rotor has affixed endplates that rotate with the central hub and vane forming a rotating spool.

- The use of dynamic sealing elements to minimize leakage between the suction and compression pockets as well as between the process pockets and the compressor containment.

The movement of the rotor is purely rotary with only the vane and tip seals performing any oscillating movement. The eccentric cam will force the movement of the vane to oscillate by twice the eccentricity during a single rotation. The tip seals will oscillate relative to the vane two times per rotation by an amount proportional to the ratio of diameters of the rotor to the housing bore. The tip seal movement amount is roughly an order of magnitude smaller than the eccentricity and follows a sinusoidal path. Analytical details regarding the geometry, including the mathematical expressions describing the chamber volumes, is presented in Bradshaw and Groll (2013).

1.1 Previous Work on the Spool Compressor

Since its introduction in 2008 the spool compressor has been improved and better understood. A comprehensive model was developed to deepen the understanding of the device holistically, as a system (Bradshaw and Groll, 2013). This
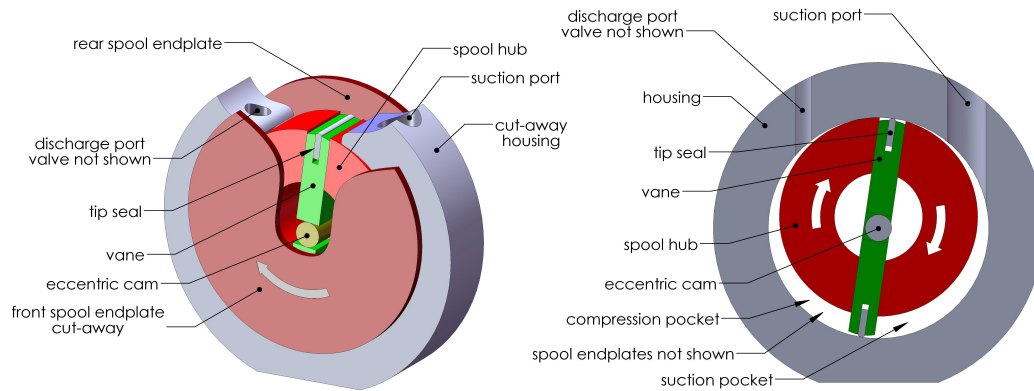
Figure 1: Cutaway view of rotating spool compressor mechanism with key components highlighted.

holistic approach has allowed for better prediction of non-intuitive behavior of the spool compressor especially applied to applications and working fluids without experimental experience. Figure 2 shows a schematic of mass and heat flows represented by the comprehensive model. The model includes 10 leak paths, 8 heat flow paths, port geometries, as well as oil solubility and frictional component sub-models.

Additionally, sub-components of the spool compressor have been studied in detail. Bradshaw (2013) presented a study on the analytical model developed to represent the tip seal in the spool compressor. The model was developed based on the tip seal dynamic model coupled with hydrodynamic lubrication theory. Kemp et al. (2012) presented iterations on the spool seal design and described the critical nature of the design of this component.

Bradshaw et al. (2016) recently presented the development of a loss analysis to describe the 5th generation spool compressor. This analysis utilized high-speed pressure measurements to determine the indicated, or flow, losses within the device. Coupled with analysis of the frictional losses an complete loss Pareto was generated. This analysis has resulted in a deep understanding of the location of potential improvements as well as an improved comprehensive modeling tool which accounts, more accurately, for the various frictional losses within the device. The resulting improvements using this analysis were also presented which showed a significant improvement in performance between the 5th and 6th generation compressor. These results echo the improved performance presented by Orosz et al. (2014).

This work will utilize the comprehensive model from Bradshaw and Groll (2013), and its improvements, to study the spool compressor operating on R134a with a variety of displacements to determine an appropriate size and shape for a R134a air-conditioning compressor. Additionally, a comparison of designs for R410A and R134a is presented which highlights the utility of the comprehensive design tool for various applications. This is accomplished by examining how the efficiencies of the compressor change with changes in the fundamental geometric parameters which define the shape of the spool compressor; the eccentricity ratio and the length-to-diameter ratio.

2. PARAMETRIC ANALYSIS

The basis of a spool compressor design starts with the selection of two quantities, the eccentricity ratio (ε), and the length to diameter ratio($^L/_D$). The eccentricity ratio is defined as,

$$\varepsilon = \frac{R_r}{R_s} \tag{1}$$

while the length to diameter ratio is defined as,

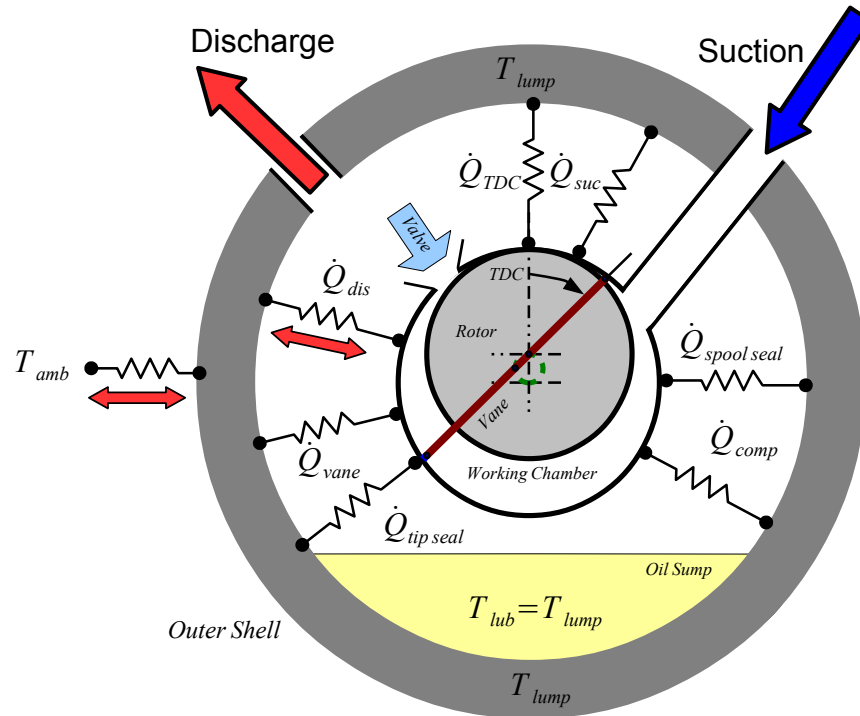$$\frac{L}{D} = \frac{h_{stator}}{2R_s}. \tag{2}$$

Figure 2: Schematic showing the mass and heat flows in the comprehensive spool compressor model as explained in Bradshaw and Groll (2013).

Figure 3 shows the basic dimensions of the spool compressor and two examples of the basic spool compressor geometry which have the same displaced volume. For a fixed displaced volume, the basic shape of the spool compressor can change depending on what values of eccentricity ratio and length to diameter ratio are selected, as shown in Figure 3.

2.1 Compressor Displacement

The eccentricity and length-to-diameter ratio are not sufficient to define a basic compressor shape, a displaced volume is also required. The displacement is a function of the working fluid and cooling capacity required at a particular operating condition. This study will compare the model predicted efficiencies of a fixed displaced volume on two working fluids, R410A and R134a, as well as 5 displaced volumes on R134a to study the influence of the displaced volume on the compressor efficiency.

For all studies the operating conditions will be fixed at an evaporating temperature of 40F (4.4C) and a condensing temperature of 100F (38C). Table 1 provides the calculated pressure ratios and calculated displaced volumes for the proposed compressors assuming a 90% volumetric efficiency. This figure represents the volume required to process the required volumetric flow rate of working fluid to generate the desired cooling capacity. This assumes an ideal refrigeration cycle with 10R (5.6K) of subcooling and 15R (8.3K) of compressor superheat. The volumetric efficiency and speed are fixed and used as an estimate though it is acknowledged that these values will vary based on operating condition and compressor geometry.

2.2 Manufacturing Considerations

One of the key leakage paths in the spool compressor is the Top Dead Center (TDC) gap. This is the gap formed by the small gap between the rotor and cylinder block. To improve leakage, and reduce manufacturing variability, the rotor is inset into the cylinder. This inset requires that a portion of the cylinder is manufactured with a discontinuous profile. The portion of the profile adjacent to the rotor is cut with a radius which is equal to the rotor. This is highlighted in Figure 4 which shows how the rotor is inset into the cylinder to increase the leakage path length of the TDC region.
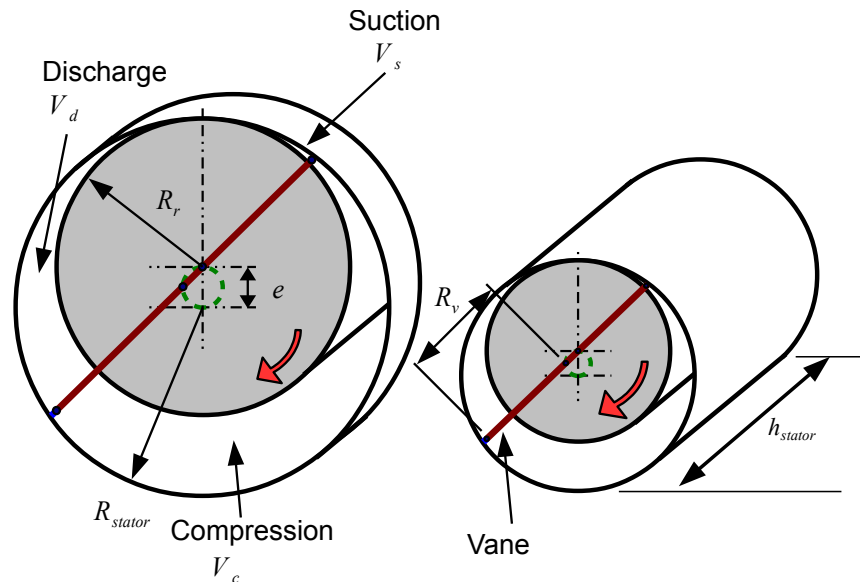
Figure 3: Spool compressor basic dimensions shown on two designs with the same displaced volume and eccentricity ratio with different length to diameter ratio.

Table 1: Table of calculated compressor displacements required to achieve various cooling loads used for study.

Fluid	PR	$\dot{Q}_{cool}$	η_{vol}	Speed	$V_{disp,tot}$	V_{disp}
-	-	tonsR (kW)	-	rpm	cm^3/rev	$cm^3/pocket$
R410A	2.49	5 (17.6)	0.9	1750	112	56
R134a	2.79	5 (17.6)	0.9	1750	254	127
R134a	2.79	20 (70.3)	0.9	1750	1014	507
R134a	2.79	40 (141)	0.9	1750	2029	1014
R134a	2.79	80 (281)	0.9	1750	4057	2029

The remaining portion of the cylinder is cut at a different radius. The section of the cylinder with the same radius as the rotor creates a region where the two components come in close contact. However, it elongates the leak path so it can be assumed the leak path is closer to two long plates in close contact opposed to a tangential line contact without this feature.

While this inset improves the leakage performance for a given compressor it is subject to the ability to manufacture the parts. This manufacturing ability changes with the eccentricity and length-to-diameter ratio selected. The length-to-diameter ratio has the most significant influence on this gap. More specifically the stator height, h_{stator}, as the stator radius has minimal influence. As the stator height increases the ability to maintain the squareness of the rotor, relative to its centerline, and the total indicated runout become more challenging. Similarly, when boring the cylinder block the ability to maintain the squareness of the TDC scallop relative to its centerline becomes more challenging as the stator height increases. The result is, for a given displacement, the TDC leakage gap will increase as the length-to-diameter increases. The amount of the deviation varies with manufacturing process used and thus is also a function of the volume of parts produced. Assuming the rotor is turned and ground and the cylinder is bored it is estimated that the TDC leakage gap will vary based on the following expression:

$$g_{TDC} = a + bh_{stator} \tag{3}$$

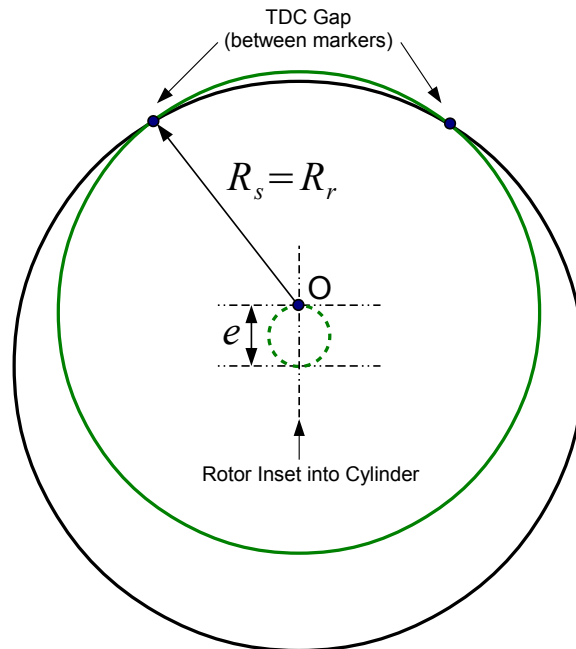where a is $0.0005in$ ($12.7\mu m$) and b is $0.0001in/in$ ($1\mu m/cm$) and h_{stator} is in inches (cm).

Figure 4: A rotor and cylinder schematic of the spool compressor highlighting the TDC region and the inset feature of the rotor into the cylinder.

3. COMPARING R410A TO R134a

Using the displaced volumes presented above in Table 1 for the 5 ton (17.3 kW) compressors a comparison between an optimum design on R410A and R134a is presented. For each displacement the model is exercised for ε values from 0.81 to 0.92 and $^L/_D$ values from 0.4 to 3 with fixed operating conditions described in Section 2.1. Figure 5 shows the overall isentropic efficiency predicted by the model for the 5 ton (17.3 kW) displacements on both R410A and R134a for all eccentricity ratios and length-to-diameter ratios.
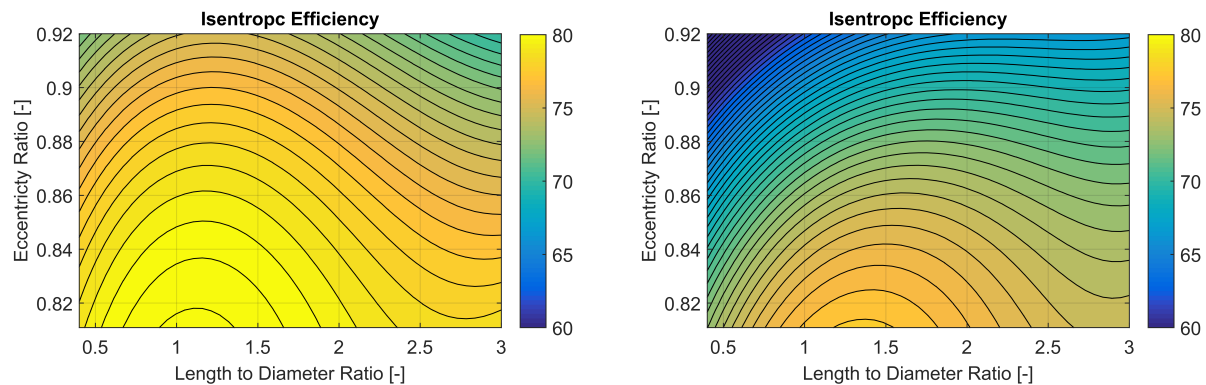

Figure 5: Overall Isentropic Efficiency of 5 ton (17.3 kW) compressor on R410A (left) and R134a (right) for various eccentricity and length-to-diameter ratios.

The overall isentropic efficiency is significantly higher for the R410A simulation at its peak (~5% points). However, it should be noted that the peak efficiency locations are at different length-to-diameter locations. For R410A the peak efficiency is predicted at length-to-diameter ratio of about 1.05 whereas the R134a peak is predicted to be at roughly 1.4 length-to-diameter ratio. Both fluids are predicted to have the highest efficiency at the lowest eccentricity possible (0.81).

Looking at the figures from the lowest eccentricity ratios to the highest there is generally a decrease in efficiency. The eccentricity ratio has minimal influence on the volumetric efficiency (i.e. leakage) so the decrease in efficiency is a result in changes of frictional losses. At the lowest eccentricity ratio the cylinder diameter (and thus spool seal) diameter is small but the movement of the vane is high. At the highest eccentricity ratio the cylinder diameter is large but the vane movement is low. These results suggest that the spool compressor is more sensitive to the spool seal friction compared with the vane friction. Therefore, based on the results here it suggests for this displacement it would be advantageous to design a compressor with the smallest eccentricity ratio possible. The R134a has a much larger range of efficiencies across a change in eccentricity ratios. This suggest the R134a design is more sensitive to changes in frictional loads compared with a R410A design.

Examining each figure from lowest length-to-diameter ratio to the highest the tradeoff between friction and leakage can be seen. At the lowest length-to-diameter ratios the cylinder diameter (and thus spool seal diameters) are forced to increase non-linearly. This creates a lot of friction per unit displacement and thus to minimize seal friction the suggestion would be to increase the length-to-diameter ratio as high as possible. However, as the length-to-diameter ratio is increased the influence of the TDC manufacturing considerations become apparent and the increase in leakage begins to overwhelm the decrease in friction. This causes a peak value within the ranges explored which is different for each fluid. For R410A the peak being lower suggests that this fluid creates an increase in sensitivity to leakage. Conversely, R134a is less sensitive to the length-to-diameter leakage which pushes the peak to a higher length-to-diameter peak value.

4. SCALING ANALYSIS

Extending the previous analysis for various displacements on R134a is presented. The displacements were previously provided in Table 1 and operating conditions defined in Section 2.1. The objective is to further understanding of the tradeoffs in design when scaling to various sizes of compressor. Figure 6 shows the results of the study of the four displaced volumes.
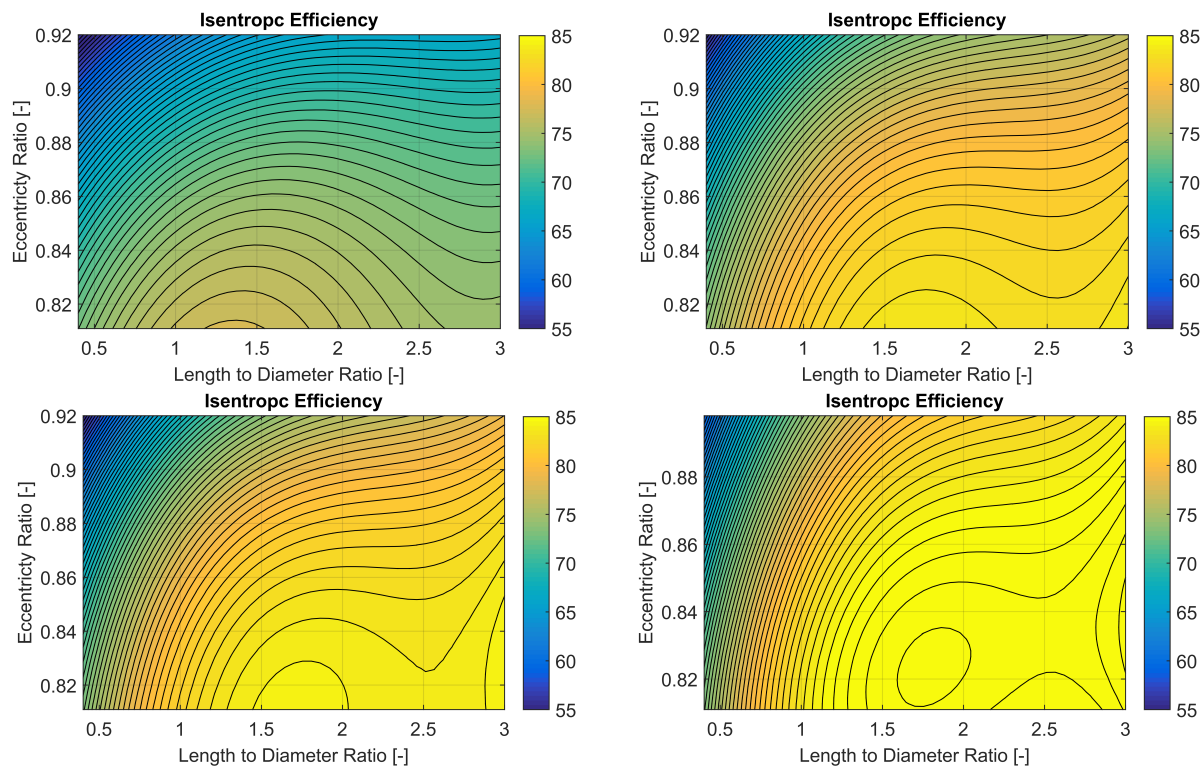

Figure 6: Overall Isentropic Efficiency of R134a compressors at 5 ton (17.3 kW), 20 ton (70.3 kW), 40 ton (141 kW), and 80 ton (281 kW) at various eccentricity and length-to-diameter ratios.

The trends are similar to the trends presented in the previous section for any given displacement. However, as the displaced volume increases the overall isentropic efficiency increases and the optimum location changes. The overall isentropic efficiency increases from a peak of roughly 77% at 5 tons (17.3 kW) to a peak of 86% at 80 tons (281 kW). This is a result of processing dis-proportionally more volume per unit frictional load as the compressor increases in displacement. While this is typical of most compressor technologies, the amount of improvement varies. The optimum location shifts from a length-to-diameter ratio of roughly 1.4 to 1.85 as the displaced volume increases. This is a result of a reduction in the sensitivity to frictional components at this displacement compared with the smaller displacements. However, as the displacement increases the peak eccentricity ratio increases, suggesting the vane friction becomes more important as the displacement increases. The peak overall isentropic efficiency and accompanying length-to-diameter ratio and eccentricity ratio are tabulated in Table 2.

Table 2: Final estimated peak efficiencies and key geometric parameters.

$\dot{Q}_{cool}$	L/D	ε	$\eta_{o,is}$
tonsR (kW)	**-**	**-**	**%**
5 (17.6)	1.4	0.81	77%
20 (70.3)	1.75	0.81	83%
40 (141)	1.82	0.815	85%
80 (281)	1.85	0.825	86%

5. DESIGN OF R134A PROTOTYPE COMPRESSOR FOR LIGHT-COMMERCIAL AIR-CONDITIONING

Using the analysis from the previous section a design for a light-commercial air-conditioning compressor is presented. The 40 ton (141 kW) size was selected as its overall isentropic efficiency is predicted to be reasonably high and the displaced volume represents a displaced volume that is difficult to find efficient products in the market. The typical alternatives, screw compressors are generally not as efficient at this displaced volume and scroll compressors are not either (Kreith, 2000).

From the data above the most efficient design for a 40 ton (141 kW) compressor is provided in Table 3.

Table 3: Final preliminary design parameters for light-commercial compressor prototype.

Parameter	Units	Value
ε	-	0.811
L/D	-	1.82
R_r	in (cm)	2.21 (5.60)
R_s	in (cm)	2.72 (6.9)
h_{stator}	in (cm)	9.890 (25.1)
$\eta_{o,is}$	%	84.6
η_{vol}	%	92.6
Discharge Temp	F (C)	128 (53.3)
Massflow	lbm/min (kg/min)	118 (53.5)
Shaft Power	kW	23.5
% Carryover Vol.	%	1.76

6. CONCLUSIONS

A design methodology utilizing a comprehensive compressor model is presented which culminates in a preliminary design of a 40 ton (141 kW) air-conditioning compressor. The study examined the utility of the approach when applied to different refrigerants as well as examining various displaced volumes. It was found that the tool provided great insight

into the appropriate basic dimensions of a compressor that would have otherwise been difficult to obtain through trial and error.

NOMENCLATURE

g_{TDC}	Gap between rotor and cylinder at TDC region	(m)
h_{stator}	Cylinder height	(m)
L/D	Length-to-diameter ratio	(-)
PR	Pressure Ratio	(-)
$\dot{Q}_{cool}$	Cooling capacity	(kW)
$\dot{Q}_{dis}$	Discharge process heat transfer	(W)
$\dot{Q}_{vane}$	Frictional loss from vane	(W)
$\dot{Q}_{tipseal}$	Frictional loss from tip seal	(W)
$\dot{Q}_{comp}$	Compression process heat transfer	(W)
$\dot{Q}_{spoolseal}$	Frictional loss from spool seal	(W)
$\dot{Q}_{suc}$	Suction process heat transfer	(W)
$\dot{Q}_{TDC}$	Frictional loss from TDC	(W)
R_r	Rotor radius	(m)
R_s	Cylinder radius	(m)
T_{amb}	Ambient temperature	(K)
T_{lub}	Lubricant temperature	(K)
T_{lump}	Compressor temperature	(K)
$V_{disp,tot}$	Total compressor displaced volume for single shaft revolution	(cm^3/rev)
V_{disp}	Compressor displaced volume for single pocket	($cm^3/pocket$)

Greek

ε	Eccentricity ratio	(-)
η_{vol}	Volumetric efficiency	(-)
$\eta_{o,is}$	Overall isentropic efficiency	(-)

REFERENCES

Bradshaw, C. (2013). Spool compressor tip seal design considerations. In *8th International Conference on Compressors and their Systems*, page 341.

Bradshaw, C. R. and Groll, E. A. (2013). A comprehensive model of a novel rotating spool compressor. *International Journal of Refrigeration*, 36(7):1974 – 1981. New Developments in Compressor Technology.

Bradshaw, C. R., Kemp, G., Orosz, J., and Groll, E. A. (2016). Development of a loss pareto for a rotating spool compressor using high-speed pressure measurements and friction analysis. *Applied Thermal Engineering*, 99:392–401.

Kemp, G., Orosz, J., Bradshaw, C., and Groll, E. A. (2012). Spool seal design and testing for the spool compressor. In *International Compressor Engineering Conference at Purdue University*, number 1259.

Kemp, G. T., Garrett, N., and Groll, E. A. (2008). Novel rotary spool compressor design and preliminary prototype performance. In *International Compressor Engineering Conference at Purdue University*, number 1328.

Kreith, F. (2000). *The CRC handbook of thermal engineering*. Springer Science & Business Media.

Orosz, J., Kemp, G., Bradshaw, C. R., and Groll, E. A. (2014). An update on the performance and operating characteristics of a novel rotating spool compressor. In *International Compressor Engineering Conference at Purdue University*, number 1378.